PERSONALIZED MODELING OF PROSTATE DEFORMATION BASED ON ELASTOGRAPHY FOR MRI-TRUS REGISTRATION

Yi Wang[1,], Dong Ni[2], Jing Qin[3], Xin Yang[2], Xiaoyan Xie[4], Muqing Lin[2], Pheng Ann Heng[1]*

[1]Department of Computer Science and Engineering, The Chinese University of Hong Kong, Hong Kong, China
[2]National-Regional Key Technology Engineering Laboratory for Medical Ultrasound, School of Medicine, Shenzhen University, China
[3]Shenzhen Institutes of Advanced Technology, Chinese Academy of Sciences, Shenzhen, China
[4]Department of Medical Ultrasonics, the First Affiliated Hospital, Institute of Diagnostic and Interventional, Sun Yat-Sen University, China

ABSTRACT

Fusion of pre- and intra-operative imaging modalities allows the accurate targeting of prostate interventions. We propose a personalized statistical motion model (PSMM) for the deformable registration of prostate magnetic resonance (MR) and 3D transrectal ultrasound (TRUS) images. Comparing to traditional statistical motion model (SMM) methods, for the first time, the biomechanical information obtained from elastography is incorporated into a finite element (FE) model, which is created from preoperative MR images. PSMM is then constructed from training data generated by simulating the prostate deformation from the personalized FE model with realistic boundary conditions. Finally, prostate MR and TRUS images are registered by integrating the PSMM into a robust point matching (RPM) framework. Using data acquired from phantoms, the efficiency of the PSMM and the accuracy of MRI-TRUS registration were evaluated. The mean target registration error was less than 1.7*mm*, which demonstrates our PSMM can achieve more physically plausible deformation estimation and accurate registration.

Index Terms— personalized modeling, elastography, prostate, statistical motion model, robust point matching, MRI-TRUS registration

1. INTRODUCTION

Prostate cancer is the most common noncutaneous cancer and the second leading cause of cancer death in men [1]. Currently transrectal ultrasound (TRUS) guided systematic biopsy is the gold standard investigation for diagnosing prostate cancer due to its real-time and radiation-free imaging capability. However, its lack of image resolution and incapability to clearly visualize early-stage prostate cancer result in false-negative rates up to 30% [2]. Therefore, by considering the higher image quality of magnetic resonance imaging (MRI), one beneficial attempt is fusing previously acquired MRI image to real-time TRUS image to provide more quality guidance, which is considered to be one of the main trends of prostate biopsy development [3].

However, efficient and accurate MRI-TRUS registration is very challenging, due to the different image appearances of these two image modalities, and the gland deformation caused by the insertion of TRUS probe. Recently statistical models have been adopted to predict the prostate deformation and register MR and TRUS images. Mohamed *et al.* [4] proposed a combined statistical model to estimate the TRUS-probe-induced prostate deformation, but the statistics of tissue properties is ignored. Dam *et al.* [5] trained prostate shape models from real segmented patient data instead of biomechanical models. However, collecting a sufficient training dataset is extremely time-consuming. Hu *et al.* [6] built a statistical motion model (SMM) for the non-rigid registration of MR and TRUS prostate images by simulating prostate motion using a finite element (FE) model, which is derived from preoperative MR images. Both tissue properties and boundary conditions were randomly sampled within a theoretical range during the simulation. However, prostates of different patients have various biomechanical properties, especially for cancerous ones which may have dramatically larger Young's modulus than normal ones. Furthermore, the composition of the prostate tissue varies between the glandular zones (central, peripheral, transition), leading to significantly different biomechanical properties of three zones [7]. As different biomechanical properties may induce totally different deformation results, this method may reduce the deformation specificity of various patients and thus limit its practical applications.

In this paper, a personalized statistical motion model (PSMM) is proposed to register preoperative prostate MR images to 3D TRUS images (Fig. 1). We first employ ultrasound elastography [7] to obtain specific biomechanical properties for personalized FE model construction. Second, PSMM is built from training data generated by simulating the prostate deformation from the personalized FE model with realistic boundary conditions, by sufficiently considering interactions of prostate, surrounding tissues, and

*Corresponding author: ywang@cse.cuhk.edu.hk

TRUS probe. Finally, we propose to non-rigidly register MR and TRUS images by integrating PSMM into a robust point matching (RPM) framework. This novel registration framework can efficiently reject outliers and achieve more physically plausible deformation estimation by making use of the advantages of both PSMM and RPM methods. To the best of our knowledge, this is the first paper to build PSMM by employing the elastography for MRI-TRUS registration.

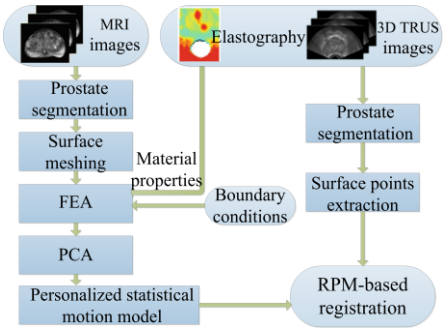

Fig. 1. The pipeline of the proposed MRI-US registration method.

2. PERSONALIZED FE MODEL

In our study, prostate gland is first manually segmented from diagnostic MR images. The segmented prostate gland is further converted into a triangulated surface mesh using adaptive skeleton climbing method [8] (Fig. 2(a)). All surface data are imported into the commercial FEA software COMSOL Multiphysics (COMSOL, LA, USA). The FE model is then meshed into tetrahedral elements by COMSOL.

In addition to the anatomical geometry, the main challenge of building biomechanical model is the assignment of proper material properties to the FE model. The nearer a physical model approaches the properties of a living tissue, the more realistic the simulation of deformations can be obtained. However, it is truly very difficult to obtain proper material properties for different anatomical zones of the prostate in practice, since the biomechanical properties of anatomical zones of the prostate are often significantly different between different zones, and vary from patient to patient. Recently, elastography has emerged as an important clinical tool for lesion detection and classification. However, little attention has been paid to employ elastography to build personalized biomechanical model for non-rigid registration. In this paper, we propose to employ the quantitative elastography to obtain the material properties instead of randomly sampling from a theoretical range [6]. Specifically, Young's modulus and Poisson's ratio are two most important biomechanical parameters for FE simulation. As Poisson's ratio of prostate is almost constant, we set v = 0.47 in our implementation. The Young's modulus of each anatomical zone of the prostate gland is obtained by averaging the Young's modulus values of each zone from previously acquired ultrasound elastography images.

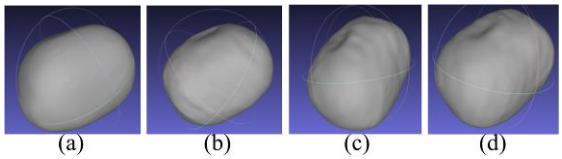

Fig. 2. Prostate surface reconstruction results, (a) MRI, (b) 3D TRUS with light deformation (US_L), (c) with median deformation (US_M), and (d) with high deformation (US_H). The deformations come from the forces of TRUS probe.

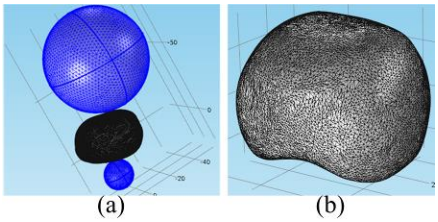

Fig. 3. (a) The geometry models in COMSOL (from top to bottom: bladder, segmented prostate and the front end of TRUS probe). (b) One typical simulation result of prostate deformation.

Table 1. Summary of the variation range of the TRUS probe used during FEA

Description	Parameter	Variation Range
Probe original position	P_x, P_y, P_z	[-5, 5] mm
Probe orientation	O_x, O_y, O_z	[-20, 20]°
Probe displacement	D_x, D_y, D_z	[5, 10] mm

3. BOUNDARY CONDITIONS

The personalized geometry and biomechanical information are the intrinsic factors determining the deformation of FE model, while surrounding structures and the placement of TRUS probe provide external restriction and force. In this regard, bladder and TRUS probe models are constructed as boundary conditions of contact and force formation.

Bladder gland is constructed in COMSOL (Fig. 3(a)) based on its shape and anatomical relationship with prostate. The bladder model is represented as a sphere because clinicians always ask patients to drink lots of water to fill the bladder before performing biopsies. The existence of the bladder model can restrict the deformation of the prostate, which is more realistic to the clinical situation.

The front end of a 3D TRUS probe is also constructed and represented as a sphere according to its physical shape. Based on the knowledge of clinicians, the variation range of the TRUS probe in terms of its pose and displacement are summarized in Table 1. The variation range is relative to the original placement of the TRUS probe.

4. PERSONALIZED STATISTICAL MOTION MODEL

A randomly sampled orientation, displacement, and position of the TRUS probe from corresponding variation ranges are set for K (=300) simulated gland deformations. One typical simulation result is illustrated in Fig. 3(b). The surface node displacements of prostate are computed based on the solid

deformation module of COMSOL. For each simulation, the *x*-, *y*-, *z*-components of the displacements of *N* surface nodes calculated by FE solver can be combined into a $3N\times1$ displacement vector **d**. Then, the PSMM **p** is calculated using principal component analysis (PCA):

$$\mathbf{p} = \mathbf{p_0} + \bar{\mathbf{d}} + \sum_{i=1}^{L} c_i \mathbf{e_i} \tag{1}$$

where $\mathbf{p}_0$ presents the original prostate position, $\bar{\mathbf{d}}$ is the average node displacement vector, $\mathbf{e}_i$ is the *i*th eigenvector of the covariance matrix of training data, c_i is weight value which determines the shape of the deformed model, and *L* is the number of principal components in the statistical model.

5. MRI-TRUS REGISTRATION

The prostate surface of the 3D TRUS is also manually segmented. Then the intersection points of 10 evenly-distributed transverse and coronal planes are generated as the sparse surface points for registration. The PSMM surface point set **p**, $\{p_i, i=1, 2, \cdots N\}$ is non-rigidly registered with the TRUS surface point set $\{q_j, j=1, 2, \cdots N'\}$ by integrating the PSMM into a RPM framework. A major advantage of RPM is that the algorithm can automatically reject a fraction of points as outliers when estimating correspondence between two point sets [9]. However, the displacement of the registered point set may not conform to the real physical situation. Therefore we extend the basic RPM framework by adding the weight value **c** from PSMM to the energy function to restrict the displacement of the registered PSMM. Given the fuzzy correspondence *M* with $\sum_{i=1}^{N+1} m_{ij} = 1$ and $\sum_{j=1}^{N'+1} m_{ij} = 1$ (m_{ij} is the probability of point *i* in p_i corresponding to point *j* in q_j), the weight value **c** of the PSMM, and the thin-plate spline (TPS) fitted function *f*, the energy function of RPM can be calculated by:

$$E(M, \mathbf{c}, f) = \sum_{j=1}^{N'}\sum_{i=1}^{N} m_{ij} \left\| q_j - f(p_i) \right\|^2 + \lambda \|Sf\| + T\sum_{j=1}^{N'}\sum_{i=1}^{N} m_{ij} \log m_{ij} - \zeta \sum_{j=1}^{N'}\sum_{i=1}^{N} m_{ij} \tag{2}$$

where p_i is constrained by weight **c**, *S* is an operator and $\|Sf\|$ is the smoothness measure, *T* is the current "temperature" which controls the iteration process of registration, λ is the smoothness coefficient, and ζ is the robustness coefficient. RPM method is an iterative process that keeps updating *M*, **c** and *f* using an annealing process; to the end, the PSMM is non-rigidly registered with TRUS data. Finally MRI and TRUS data are registered together according to the deformation field provided by FEA and the corresponding relationship between MRI data and PSMM.

6. EXPERIMENTAL RESULTS

In order to verify our method, experiments were carried on the datasets obtained from two different commercial prostate phantoms 053-MM and 053-AEF (CIRS, Norfolk, USA). MRI images were acquired using a 3.0 Tesla MR-scanner (Magnetom Trio; Siemens, Erlangen, Germany) with a 32 channels head coil. The TRUS and ultrasound elastography images were obtained respectively by DC-8 (Mindray, Shenzhen, China) and Aixplorer (Supersonic, France) ultrasound system. Fig. 4 shows different modalities of 053-MM images. It is worth noting that the average Young's modulus (E = 30kPa and 20kPa for 053-MM and 053-AEF respectively) of prostate obtained from the elastography is assigned to the corresponding FE models, due to the isotropic biomechanical properties of both phantoms.

In order to demonstrate the advantages of our method, the efficiency of PSMM was first evaluated by two metrics: model compactness and generalization ability, which represent the relative cumulative variance and the ability of representing unknown test data, respectively. The generalization ability of PSMM was compared with that of the traditional SMM constructed from training data with same FEA setting, except without using specific Young's modulus (randomly sampled within (E: [5, 50]kPa)). Then the accuracy of MRI-TRUS registration by our proposed method was calculated and compared with that of SMM by evaluating target registration error (TRE).

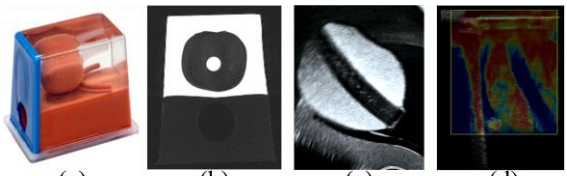

Fig. 4. Various imaging modalities: (a) model 053-MM: (b) transverse MRI-T2 image, (c) B-mode ultrasound, and (d) ultrasound elastography.

6.1. Personalized Statistical Motion Model Evaluation

Model compactness *C* can be calculated as:

$$C(L) = \sum_{i=1}^{L} \lambda_i \Big/ \sum_{j=1}^{K} \lambda_j \tag{3}$$

where λ_i is the *i*th eigenvalue of the covariance matrix of the training data. The average compactness of the PSMM constructed from 053-MM and 053-AEF is very close to 1.0 when $L \geq 10$, which demonstrates our model has good compactness property.

Model generalization ability is defined as the average root-mean-square (RMS) of the corresponding node distance between model and test data. For each of 300 repeated times, PSMM is constructed using 299 simulated data and fitted to the remaining data. The average RMS values by PSMM were 0.24±0.06*mm* and 0.28±0.06*mm* respectively for 053-AEF and 053-MM, and the corresponding values by SMM were 0.33±0.09*mm* and 0.35±0.11*mm* respectively. It

indicates that a model with accurate biomechanical properties is essential for training the deformable model.

6.2. MRI-TRUS Registration Results

We evaluated registration results on MRI images and various deformed TRUS data of the same phantom (Fig. 2(b)-(d)). The deformation mainly comes from forces of TRUS probe. The RPM based registration can be performed within 13*s* using a PC with 2.30 GHz Intel (R) Core (TM) dual CPU and 2.0 GB RAM.

Each prostate phantom contains three 5-10*mm* quasi-sphere lesions; consequently, the leftmost, rightmost, top, bottom, foremost and rearmost points of each lesion relative to global phantom coordinate were manually extracted from MRI and TRUS data as landmarks to evaluate registration accuracy. The total 18 landmarks from MRI were transformed into the TRUS space and TREs were calculated. Fig. 5 illustrates the registered MR image and corresponding target TRUS image. Table. 2 shows that PSMM can represent deformation more accurately when comparing to SMM. Registration results on various TRUS data achieved by using PSMM are all better than those of SMM. The average TRE of PSMM was less than 1.7*mm*. The deformation can be compensated for nearly 60% by using PSMM. However, the TREs on high deformed TRUS are still distinctly larger than ones with light deformations. This is expected to be improved by using some local surface registration schemes.

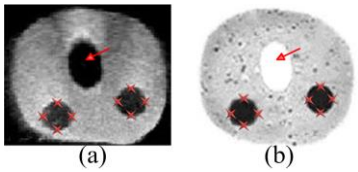

Fig. 5. (a) Transverse TRUS image and (b) corresponding MR image following non-rigid registration. The cross marks indicate corresponding landmarks which were well aligned. The arrows point to urethra region.

Table 2. Target registration error (TRE) for selected landmarks

Dataset		Mean ± SD TRE in *mm*			
		US_L	US_M	US_H	All
053 MM	Start	3.14±0.50	4.24±0.45	5.96±0.58	4.45±1.27
	SMM	1.80±0.13	2.05±0.27	2.31±0.35	2.05±0.34
	PSMM	1.40±0.16	1.62±0.28	1.99±0.25	1.67±0.32
053 AEF	Start	2.89±0.35	4.02±0.45	5.18±0.91	4.03±1.12
	SMM	1.92±0.22	2.14±0.32	2.33±0.42	2.13±0.36
	PSMM	1.50±0.20	1.60±0.29	1.98±0.40	1.69±0.37

7. CONCLUSION

In this paper, we present a novel PSMM for registration of prostate MRI-TURS images. Comparing to traditional SMM methods, we, for the first time, introduce patient-specific biomechanical properties provided by elastography into FEA, which can make the deformable model more accurate and practical for clinical applications. In addition to prostate, our personalized deformation modeling method can also be applied to other organs. We further propose a non-rigid registration method by integrating a PSMM into RPM framework, which can efficiently reject outliers and achieve more physically plausible deformation estimation. Experimental results on two different phantoms illustrate that the proposed model has better ability to capture the prostate deformation, and the registration accuracy by the proposed method is improved comparing with that by SMM method. In the future, the proposed method will be applied and evaluated on real patient data. Advanced local registration scheme will also be implemented to deal with large deformations.

8. ACKNOWLEDGMENTS

This work described in this paper was supported in part by a grant from the Research Grants Council of Hong Kong (No. CUHK 412510), in part by a grant from Shenzhen-Hong Kong Innovation Circle Funding Program (No. JSE201109150013A), in part by a grant from Chinese Postdoctoral Science Foundation (No. 2013M530372).

9. REFERENCES

[1] R. Siegel, D. Naishadham, and A. Jemal, "Cancer statistics, 2013," *CA Cancer J Clin*, vol. 63, pp. 11–30, 2013.

[2] G. Guichard, S. Larré, A. Gallina, A. Lazar, H. Faucon, S. Chemama, Y. Allory, J. Patard, D. Vordos, and A. Hoznek, "Extended 21-sample needle biopsy protocol for diagnosis of prostate cancer in 1000 consecutive patients," *Eur Urol*, vol. 52, pp. 430–435, 2007.

[3] H.U. Ahmed, A. Kirkham, M. Arya, R. Illing, A. Freeman, C. Allen, and M. Emberton, "Is it time to consider a role for MRI before prostate biopsy," *Nat Rev Clin Oncol*, vol. 6, pp. 197-206, 2009.

[4] A. Mohamed, C. Davatzikos, and R. Taylor, "A combined statistical and biomechanical model for estimation of intra-operative prostate deformation," *MICCAI*, vol. LNCS 2489, pp. 452-460, 2002.

[5] E. Dam, P.T. Fletcher, S.M. Pizer, G. Tracton, and J. Rosenman, "Prostate shape modeling based on principal geodesic analysis bootstrapping," *MICCAI*, vol. LNCS 3217, pp. 1008-1016, 2004.

[6] Y. Hu, H.U. Ahmed, Z. Taylor, C. Allen, M. Emberton, D. Hawkes, and D. Barratt, "MR to ultrasound registration for image-guided prostate interventions," *Med Image Anal*, vol. 16, pp. 687-703, 2012.

[7] J.M. Correas, A.M. Tissier, A. Khairoune, G. Khoury, D. Eiss, and O. Helenon, "Ultrasound elastography of the prostate: state of the art," *Diagn Interv Imaging*, vol. 94, pp. 551-560, 2013.

[8] T. Poston, T.T. Wong, and P.A. Heng, "Multiresolution isosurface extraction with adaptive skeleton climbing," *Computer Graphics Forum*, vol. 17, pp. 137-148, 1998.

[9] H. Chui, and A. Rangarajan, "A new point matching algorithm for non-rigid registration," *CVIU*, vol. 89, pp. 114-141, 2003.